

Recognition by a Solubilized Receptor: Hydrogen Bonding, Solvophobic Interactions, and Solvent Engineering inside Micelles

Richard P. Bonar-Law

Contribution from the Cambridge Centre for Molecular Recognition, University Chemical Laboratory, Lensfield Road, Cambridge CB2 1EW, U.K.

Received July 17, 1995*

Abstract: This paper shows how a hydrophobic porphyrin-based receptor capable of multipoint recognition in organic solvents can be solubilized directly in water by incorporation inside micelles. Binding of ligands from the aqueous phase is analyzed in sodium dodecylsulphate (SDS) micelles using a simple model in which ligands first partition into the micelle and are then complexed by the receptor. Subtraction of ligand-micelle partitioning terms from observed binding energies gives energies for bimolecular association inside SDS micelles, which range from +1 to -22 kJ/mol (equilibrium constants from 0.7 to 7900 M⁻¹). Comparison of two receptors binding the same set of ligands in SDS and organic solvents then provides insight into the roles of ligand and receptor solvation in micellar recognition. Binding inside SDS micelles is found to be energetically similar to binding in methanol, in that hydrogen bonding in the SDS pseudophase is reduced relative to CH₂Cl₂, and association of ligands capable of nonpolar contacts with the receptor is enhanced. Micellar recognition is most effective when both hydrogen bonding and solvophobic forces act together, leading to increased chiral discrimination of hydrophobic amino acid derivatives. It is finally shown how receptor solvation inside micelles can be tuned by the addition of organic cosolvents, reducing solvophobic association and restoring some of the hydrogen bonding energy.

Introduction

Although directed hydrogen bonds can be a powerful driving force for molecular recognition in nonpolar solvents,¹ hydrogen bonds are weak in water unless they are part of a cooperative array.² Hence artificial receptors for neutral species in water typically employ only solvophobic and dispersive forces.³ These interactions are relatively nondirectional, so *selective* recognition requires synthesis of a precisely sculpted receptor which follows the contours of the ligand closely.⁴ A simple alternative strategy is to solubilize a hydrogen bonding receptor directly in water by coating it with a layer of surfactant. Incorporating the receptor inside a micelle⁵ in this fashion has the advantage of shielding the active site from bulk water and also bypasses the need to incorporate solubilizing functionality during synthesis. The main disadvantage is that one is no longer dealing with a discrete molecule but a dynamic supramolecular assembly whose usefulness may be restricted, e.g., to a particular range of surfactant concentrations. Nowick et al. were the first to

investigate hydrogen bonded association inside micelles, measuring the base-pairing of adenine and thymine derivatives in surfactant solution.^{6a-c} Jursic has also shown that chiral mixed micelles derived from amide-based surfactants can form diastereomeric complexes with a chiral amide solute.^{6d} Other examples of bimolecular association inside micelles include measurements of pK_as and rates of metalation of micellar porphyrins⁷ and studies of micelle-solubilized iron porphyrins as mimics of haeme-containing proteins.⁸

Initially inspired by the solubilization of C₆₀ in aqueous surfactants,⁹ this paper explores the recognition properties of the large hydrophobic receptor **1** solubilized inside micelles. **1** is composed of a porphyrin capped on both faces with a steroidal superstructure which acts as a chiral recognition site.^{10,11} In nonpolar solvents **1** binds a variety of species by a combination of Lewis acid coordination to the zinc atom, hydrogen-bonding

* Abstract published in *Advance ACS Abstracts*, December 1, 1995.

(1) (a) For recent examples see *Tetrahedron* **1995**, *51*, 343–648. (b) Wintner, E. A.; Conn, M. M.; Rebek, J., Jr. *Acc. Chem. Res.* **1994**, *27*, 198. (c) Webb, T. H.; Wilcox, C. S. *Chem. Soc. Rev.* **1993**, 383.

(2) Crieghton, J. E. *Proteins: structures and molecular properties*; W. H. Freeman: New York, 1993; pp 165–167.

(3) For notable exceptions see: (a) Torneiro, M.; Still, W. C. *J. Am. Chem. Soc.* **1995**, *117*, 5887. (b) Kato, Y.; Conn, M. M.; Rebek, J., Jr. *Proc. Natl. Acad. Sci. U.S.A.* **1995**, *92*, 1208. (c) Kobayashi, K.; Asakawa, Y.; Kato, Y.; Aoyama, Y. *J. Am. Chem. Soc.* **1992**, *114*, 3285.

(4) (a) Peterson, B. R.; Mordasini-Denti, T.; Diederich, F. *Chem. Biol.* **1995**, *2*, 139. (b) Adrian, J. C., Jr.; Wilcox, C. S. *J. Am. Chem. Soc.* **1992**, *114*, 1398.

(5) For leading references to micelle chemistry see: (a) Myers, D. *Surfactant Science and Technology*; VCH: Weinheim, 1992. (b) Hunter, R. J. *Foundations of Colloid Science*; Clarendon: Oxford, 1987. (c) Fendler, J. H. *Membrane Mimetic Chemistry*; Wiley: New York, 1982. (d) *Solution Chemistry of Surfactants*; Mittal, K. L., Ed.; Plenum: New York, 1979. (e) *Micellization, Solubilization and Microemulsions*; Mittal, K. L., Ed.; Plenum: New York, 1976. (f) Fendler, J. H.; Fendler, E. J. *Catalysis in Micellar and Macromolecular Systems*; Academic: New York, 1975. (g) Menger, F. M. *Acc. Chem. Res.* **1979**, *12*, 111.

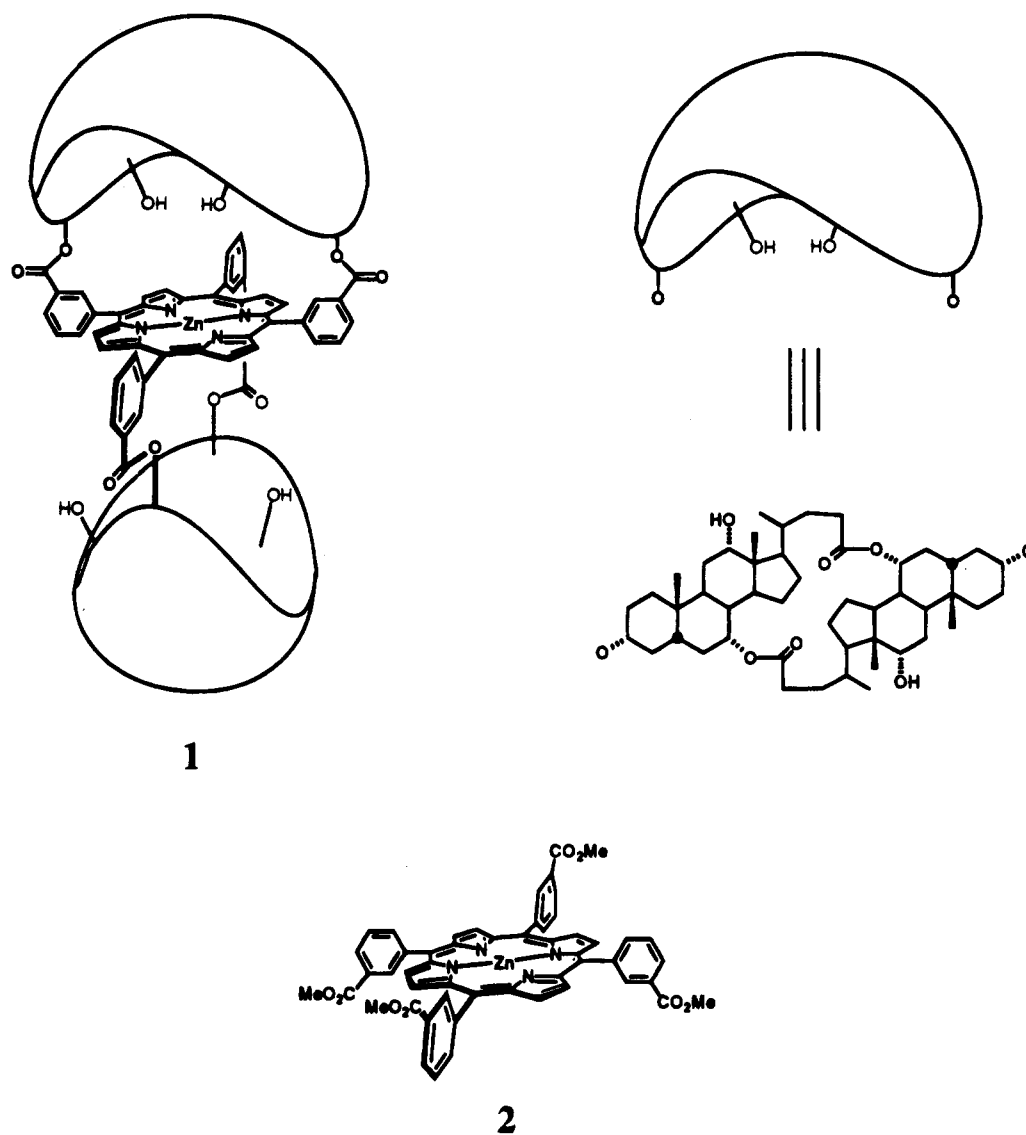
(6) (a) Nowick, J. S.; Cao, T.; Noronha, G. *J. Am. Chem. Soc.* **1994**, *116*, 3285. (b) Nowick, J. S.; Chen, J. S.; Noronha, G. *J. Am. Chem. Soc.* **1993**, *115*, 7636. (c) Nowick, J. S.; Chen, J. S. *J. Am. Chem. Soc.* **1992**, *114*, 1107. (d) Jursic, B. S. *Tetrahedron Lett.* **1993**, *34*, 963.

(7) (a) Barber, D. C.; Woodhouse, T. E.; Whitten, D. G. *J. Phys. Chem.* **1992**, *96*, 5106. (b) Barber, D. C.; Freitag-Beeston, R. A.; Whitten, D. G. *J. Phys. Chem.* **1991**, *95*, 4074. (c) Rao, V. H.; Krishnan, V. *Inorg. Chem.* **1985**, *24*, 3538. (d) Williams, G. N.; Williams, R. F. X.; Lewis, A.; Hambright, P. *J. Inorg. Nucl. Chem.* **1979**, *41*, 41. (e) Lowe, M. B.; Phillips, J. N. *Nature* **1962**, *194*, 1058.

(8) (a) Mazumdar, S. *J. Chem. Soc., Dalton Trans.* **1991**, 2091. (b) Mazumdar, S. *J. Phys. Chem.* **1990**, *94*, 5947. (c) Mazumdar, S.; Mehdi, O. K.; Mitra, S. *J. Chem. Soc., Dalton Trans.* **1990**, 1057. (d) Mazumdar, S.; Mehdi, O. K.; Kannadagulli, N.; Mitra, S. *J. Chem. Soc., Dalton Trans.* **1989**, 1003. (e) Mazumdar, S.; Mehdi, O. K.; Mitra, S. *Inorg. Chem.* **1988**, *27*, 1057. (f) Minch, M. J.; LaMar, G. N. *J. Phys. Chem.* **1982**, *86*, 1400. (g) Traylor, T. G.; Chang, C. K.; Geibel, J.; Berzins, A.; Mincey, T.; Cannon, J. *J. Am. Chem. Soc.* **1979**, *101*, 6716. (h) Hambright, P.; Chock, P. B. *J. Inorg. Nucl. Chem.* **1975**, *37*, 2363. (i) Simplicio, J.; Schwenzer, K. Maenpa, F. *J. Am. Chem. Soc.* **1975**, *97*, 7319. (j) Simplicio, J.; Schwenzer, K. *Biochemistry* **1973**, *12*, 1923. (k) Simplicio, J. *J. Biochem.* **1972**, *11*, 2525.

(9) (a) Bensasson, R. V.; Bienvenue, E.; Dellinger, M.; Leach, S.; Seta, P. *J. Phys. Chem.* **1994**, *98*, 3492. (b) Beedy, A.; Eastoe, J.; Heenan, R. K. *J. Chem. Soc., Chem. Commun.* **1994**, 173. (c) Hungerbühler, H.; Guld, D. M.; Asmus, K.-D. *J. Am. Chem. Soc.* **1993**, *115*, 3386.

Chart 1



to the inwardly pointing hydroxyl groups and dispersive attraction to the hydrocarbon underside of the roof.^{10a} **1** seemed particularly suitable for a solubilization approach because (1) the hydrophobic roof should fix the receptor firmly in the nonpolar core of the micelle, (2) the roof should protect the binding site to some extent from intrusion of surfactant molecules, (3) the porphyrin chromophore can provide both a probe of receptor environment and a sensor for ligand recognition, and (4) this receptor employs three types of binding force, all of which may be modulated in a micellar environment, leading to unique binding selectivity.

The spectroscopic and ligand binding properties of **1** and also **2**, which serves as a reference for **1**, are initially compared in a variety of surfactants. A simple model for intramicellar coordination is developed, and binding energies in sodium dodecylsulfate (SDS) micelles and organic solvents are compared. Binding in micelles is shown to be similar to binding in methanol in energetic terms, although there are differences in receptor solvation. In keeping with the methanol analogy, hydrogen bonding is weaker in SDS relative to CH_2Cl_2 , and

solvophobic binding is stronger. This leads to changes in overall ligand selectivity compared to CH_2Cl_2 , including increased chiral discrimination of some amino acid derivatives. Finally, it is shown how the scope of micellar receptors can be extended by doping with organic solvents, reducing the solvophobic force and restoring some of the hydrogen bonding energy.

Results and Discussion

Initial Comparisons of Spectroscopic and Ligand Binding Properties of 1 and 2 in Different Surfactants. The Solvent Environment inside Micelles. To find a system suitable for quantitative analysis of coordination to zinc porphyrins inside micelles, a selection of anionic, cationic, and neutral surfactants was initially screened for solubilization of **1** and **2** in water, Table 1. A ratio of $[\text{surfactant}]/[\text{porphyrin}] = 2 \times 10^4$ was used to ensure only one porphyrin per micelle (see Experimental Section).

The Soret bands of **1** and **2** inside micelles are red shifted and broadened compared to CH_2Cl_2 , a typical nonpolar solvent, Table 1. Coordination of donor solvents to the zinc atom of zinc porphyrins induces red shifts,^{12,13a} and a method of distinguishing this type of red shift from general medium effects

(10) (a) Bonar-Law, R. P.; Sanders, J. K. M. *J. Chem. Soc., Chem. Commun.* **1991**, 574. (b) Bonar-Law, R. P.; Sanders, J. K. M. *J. Am. Chem. Soc.* **1995**, *117*, 259.

(11) For a review of steroid-based receptors see: Davis, A. P. *Chem. Soc. Rev.* **1993**, 243.

(12) Kolling, O. W. *Inorg. Chem.* **1979**, *18*, 1175.

Table 1. UV Characteristics of **1** and **2** and Pyridine Binding Constants (K_{obs} , M^{-1}) in Different Surfactants and Solvents

	1				2			
	λ_{max} ($W_{1/2}$) ^a	$\Delta\lambda_{\text{max}}$ ($\pm\text{Zn}$) ^b	$\Delta\lambda_{\text{max}}$ ($\text{Zn} \pm \text{Py}$) ^c	K_{obs} ^d	λ_{max} ($W_{1/2}$)	$\Delta\lambda_{\text{max}}$ ($\pm\text{Zn}$)	$\Delta\lambda_{\text{max}}$ ($\pm\text{Py}$)	K_{obs}
SDS ^e	429.5 (11.3)	6.0	5.5	7.9×10^3	426.3 (8.5)	7.8	4.0	123
NaDC	434.0 (15.5)	6.0	2.5	1.4×10^3	429.5 (8.8)	9.0	1.5	443
TTAB	432.0 (15.0)	8.0	3.5	2.5×10^3	428.0 (8.8)	9.0	2.5	87
CPC	432.5 (15.5)	8.0	4.5	945	429.3 (10.5)	9.8	1.5	32
Triton X-100	436.0 (11.0)	8.8	2.0	5	429.0 (8.8)	9.5	1.5	134
MeOH	429.5 (10.0)	9.5	3.5	11	422.8 (8.0)	9.0	3.5	5
wet CH_2Cl_2 ^f	430.5 (12.0)	6.0	5.0	3.6×10^3	421.0 (11.8)	2.5	8.5	1.3×10^4
CH_2Cl_2	426.0 (11.3)	1.5	9.5	1.6×10^4	420.0 (9.5)	1.5	9.5	2.0×10^4

^a λ_{max} of Soret (width at half height), measured in 30 mM surfactant (± 0.25 nm). Porphyrin solutions prepared in 100 mM surfactant at a surfactant/porphyrin ratio $R = 2 \times 10^4$. ^b $\Delta\lambda_{\text{max}}(\pm\text{Zn}) = \lambda_{\text{max}}(\text{zinc porphyrin}) - \lambda_{\text{max}}(\text{free base porphyrin})$. ^c $\Delta\lambda_{\text{max}}(\text{Zn} \pm \text{Py}) = \Delta\lambda_{\text{max}}(\text{zinc porphyrin} + \text{pyridine}) - \Delta\lambda_{\text{max}}(\text{zinc porphyrin})$. ^d Measured by UV titration at 295 K in 30 mM surfactant (10 mM pH 7 buffer) or in dry organic solvent. ^e SDS = sodium dodecylsulfate, NaDC = sodium deoxycholate, TTAB = tetradecyltrimethylammonium bromide, CPC = cetylpyridinium chloride, Triton X-100 = $p\text{-(CH}_3)_3\text{CCH}_2\text{C(CH}_3)_2\text{C}_6\text{H}_4\text{O(CH}_2\text{CH}_2\text{O)}_n\text{CH}_2\text{CH}_2\text{OH}$. ^f CH_2Cl_2 containing ~ 0.1 M water.

on UV transitions is to plot the Soret λ_{max} in a variety of solvents against $(n^2 - 1)/(2n^2 + 1)$, a measure of solvent polarizability, where n is the solvent refractive index.¹³ Soret λ_{max} values for **1** and **2**, their pyridine complexes **1**·pyridine and **2**·pyridine, and free base porphyrins **H**₂**1** and **H**₂**2** are displayed in Figure 1, with red shifts in surfactants tabulated as $\Delta\lambda_{\text{max}}$ values in Table 1. Three general points can be made.

(1) The differences between λ_{max} values for zinc and free base porphyrins inside micelles (top sections of Figure 1A,B) are similar to those of donor solvents (bottom of Figure 1A,B). This implies that the zinc atoms of **1** and **2** bear axial ligands in micelles. The scatter in the organic solvent correlations for capped porphyrins is due the additional effects of cavity solvation, discussed further below.

(2) The relative λ_{max} values for **1** and **2** in micelles and organic solvents are similar implying that **1** and **2** are solubilized in similar locations.

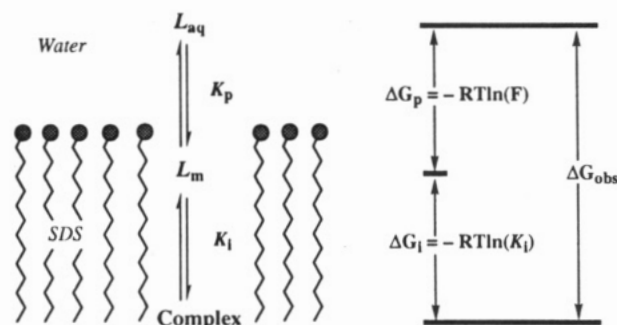
(3) The λ_{max} values for free base porphyrins and zinc-pyridine adducts in micelles are comparable to λ_{max} values in chlorinated and aromatic solvents respectively, implying that **1** and **2** experience a polarizable organic-like microenvironment inside micelles.

As a further probe of receptor environment equilibrium constants (K_{obs}) were measured for pyridine binding to **1** and **2** in different surfactants by UV-visible titration, Table 1. K_{obs} values describe the overall transfer of pyridine from water, through the micellar coat and onto the zinc atom. Titrations gave sharp isosbestic points and were well fitted by 1:1 binding isotherms. A typical SDS titration is shown in Figure 2. K_{obs} values are 30–60-fold larger for **1** than **2** in long-chain charged surfactants, 3-fold larger in the steroidal surfactant NaDC, and 30-fold smaller in the neutral surfactant Triton X-100. Reduced binding to **1** relative to **2** could be due to more effective competition for its binding site by surfactant head groups or water. Competition by the charged surfactants seems unlikely since, with the exception of NaDC, these form well defined aggregates with the head groups pointing outwards.⁵ However neutral micelles of Triton X-100¹⁴ are probably less well ordered and may allow polyether head groups to sample the micellar interior; indeed UV titration showed that Triton X-100 does bind more strongly to **1** than **2** in CH_2Cl_2 .¹⁵ Assuming that

charged surfactants do not coordinate then, by default, water must be responsible for the red shifts in Figure 1.¹⁶ Judging from greater reduction in K_{obs} for **1** in wet CH_2Cl_2 compared to dry CH_2Cl_2 (Table 1), water binds more strongly to **1** than **2** in a nonpolar solvent.^{10b} Comparison of λ_{max} s in wet CH_2Cl_2 and SDS suggests that water also binds more strongly to **1** than **2** in micelles. Water is well-known to coordinate to iron porphyrins inside micelles.⁸

In summary, UV shifts and ligand binding comparisons suggest that in charged micelles the metal sites in **1** and **2** are partially saturated, probably by water. By analogy with a ¹³C NMR study of octaethylporphyrin in SDS,^{8a} **1** and **2** are assumed to reside in the core of micelles, consistent with the nonpolar nature of the porphyrin microenvironment. SDS was chosen for further study because the binding site of **1** appeared to be least affected by this surfactant.

A Binding Model. Binding is treated within the pseudophase approximation^{17,18} as a two stage process^{6b} in which a ligand partitions from aqueous solution into the micellar phase with partition coefficient $K_p = L_m/L_{\text{aq}}$ and then binds to the receptor with equilibrium constant K_i (see Appendix). The experimen-



tally measured equilibrium constant is related to K_i by $K_{\text{obs}} = FK_i$ where F is the factor by which ligand is concentrated in receptor-containing micelles from bulk solution. The observed binding energy is then the sum of partitioning and intramolecular terms.

(16) Opinions differ about the wetness of micellar interiors, for leading references see: Menger, F. M.; Mounier, C. E. *J. Am. Chem. Soc.* **1993**, *115*, 12222. Neutron diffraction of SDS micelles gives less than one water per surfactant chain in the hydrocarbon interior, ref 24.

(17) (a) Mukerjee, P. in ref 5d, Vol. 1, p 153. (b) Bunton, C. A. in ref 5d, Vol. 2, p 519. (c) Romstead, L. S. in ref 5e, Vol. 2, p 509. (d) Martinek, K.; Yatsimirski, A. K.; Osipov, A. P.; Berezin, I. V. *Tetrahedron*, **1973**, *29*, 963. (e) Elworthy, P. H.; Florence, A. T.; McFarlane, C. B. *Solubilization by Surface Active Agents, and Its Application in Chemistry and the Biological Sciences*; Chapman and Hall: London, 1968.

(18) Micelle-ligand binding can be treated equally well as a multiple association process: De Lisi, R.; Liveri, V. T. *Gazz. Chim. Ital.* **1983**, *113*, 371.

(13) (a) Nappa, M.; Valentine, J. S. *J. Am. Chem. Soc.* **1978**, *100*, 5075. (b) Reichardt, C. *Solvents and Solvent Effects in Organic Chemistry*; VCH: Weinheim, 1988; p 295.

(14) Matsuura, H.; Fukuhara, K.; Takashima, K.; Sakakibara, M. *J. Phys. Chem.* **1991**, *95*, 10800.

(15) For Triton X-100 in CH_2Cl_2 , $K_1 = 183 \text{ M}^{-1}$ and $K_2 = 74 \text{ M}^{-1}$. SDS or NaDC did not bind appreciably to **1** or **2** in CH_2Cl_2 or methanol. TTAB and CPC bind in CH_2Cl_2 , but the process being monitored by UV titration is coordination of the halide counteranions. For CPC, $K_1 = 563 \text{ M}^{-1}$ and $K_2 = 4.9 \times 10^3 \text{ M}^{-1}$.

$$\Delta G_{\text{obs}} = \Delta G_p + \Delta G_i = -RT \ln (FK_i) \quad (1)$$

Equilibrium constants were typically measured with a large excess of micelles over receptor so that the concentration factor assumes the simple form $F = K_p / (1 + ([\text{SDS}] - \text{cmc})v^m(K_p - 1))$ where $\text{cmc} = 8 \text{ mM}$ is the critical micelle concentration of SDS and $v^m = 0.25 \text{ L/mol}^{19}$ is the molar volume of SDS in water. Ligand partition coefficients were determined by micellar capillary electrophoresis.²⁰

Titration with ligands **L1**–**L9** were fitted well by 1:1 binding isotherms, suggesting that K_p remains constant up to the point of receptor saturation. However binding curves for the hydrophobic ligand **L11**, and to a lesser extent **L10**, flattened sooner than expected at high ligand concentrations. This may be due to a reduction in K_p as micelle saturation is approached,²¹ most noticeable for **L11** because micelles have low capacities for bulky hydrophobic species,²² and this ligand binds particularly weakly, requiring high intracellular concentrations. To allow for this effect, curve fitting of binding isotherms for **L10** and **L11** was restricted to 0–50% receptor saturation.

Equilibrium was established in less than 1 min after addition of **L1** to **L11** to micellar porphyrins showing that exchange of small ligands between micelles is rapid.^{22b} **L12** was prepared as a counterexample to see how hydrophobic a ligand needs to be before intermicellar exchange becomes slow. Although **L12** binds rapidly in organic solvents, equilibrium was attained only gradually in SDS, with a half-life of 2.5 h.

Comparison of 1 and 2 in SDS. Porphyrin **2** was to be used as a reference for **1**, so it was important to have a quantitative estimate of how the different sizes²³ of **1** and **2** might affect the ligand-binding properties of porphyrin-containing micelles. Pyridine binding energies are plotted in Figure 3 as a function of increasing SDS concentration for fixed concentrations (1 μM) of **1** and **2**, along with the predicted behaviors from eq 1 (solid lines).²⁵ Porphyrin **2** behaves largely as expected, but **1** binds pyridine more strongly than predicted at high surfactant concentrations. This trend was observed for most of the ligands examined as shown in Figure 4, where the difference between binding energies at 30 and 100 mM SDS is compared with the difference calculated from eq 1, using the experimentally determined K_p values in Table 2. The origin of the stronger binding by **1** is not known, but may be due to an increase in K_p and/or K_i as micelles become slightly larger at high SDS concentrations.²⁶

The constant energy differences for **L1**–**L9** in Figure 4 confirms that the micellar binding site around both porphyrins is realistically modeled as a single phase for moderately polar

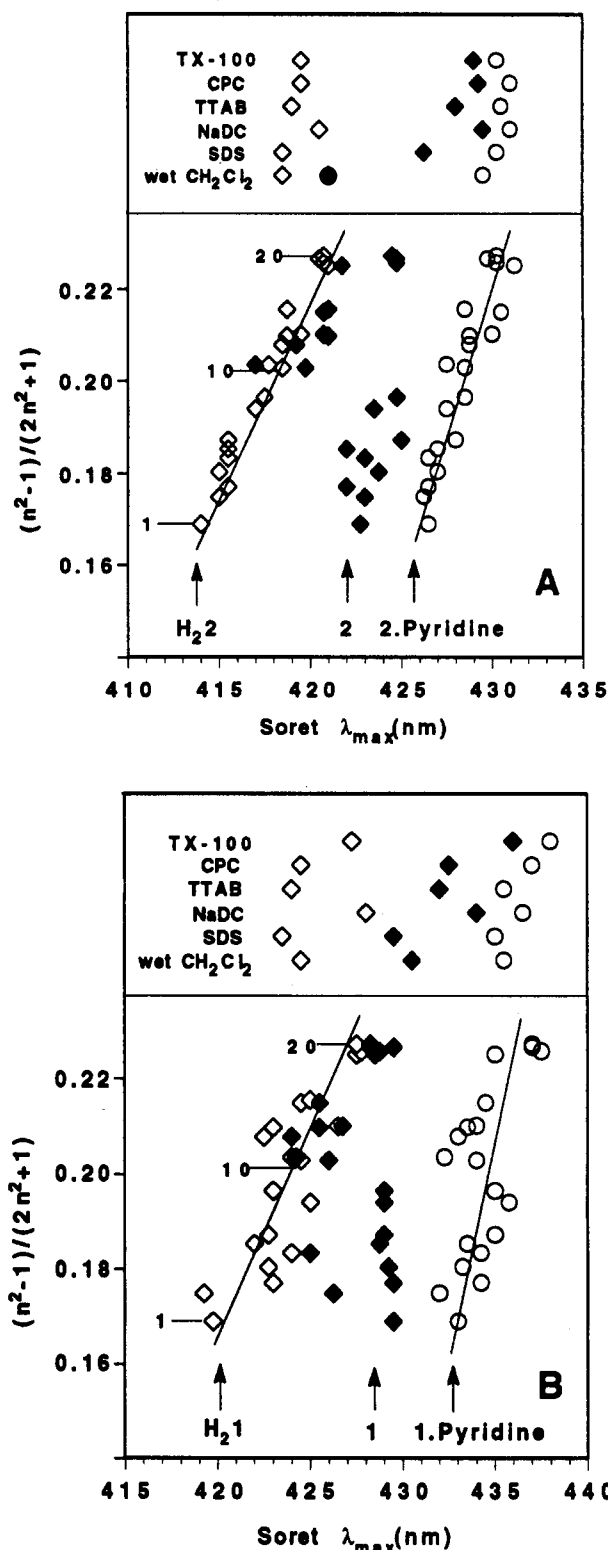


Figure 1. (A) $(n^2 - 1)/(2n^2 + 1)$ versus Soret λ_{max} for free base porphyrin **H22**, zinc porphyrin **2** and the 2-pyridine complex in neat solvents (bottom section) and surfactants (top section). Soret λ_{max} values in surfactants are grouped together for comparison and are not on any vertical scale. The lines are least squares fits, $R = 0.98$ for **H22**, $R = 0.92$ for 2-pyridine. (B) Same plot for capped porphyrins, $R = 0.86$ for **H21**, and $R = 0.62$ for 1-pyridine. For surfactant abbreviations see Table 1. Solvents in ascending order: 1, methanol; 2, acetonitrile; 3, diethyl ether; 4 acetone; 5, diisopropyl ether; 6, ethyl acetate; 7, isopropyl alcohol; 8, dibutyl ether; 9, THF; 10, dichloromethane; 11, cyclohexane; 12, 1,1,1-trichloroethane; 13, 1,2-dichloroethane; 14, chloroform; 15, tetrachloromethane; 16, chlorocyclohexane; 17, 1,1,1,2,2-tetrachloroethane; 18, toluene; 19, mesitylene; 20, benzene.

(19) Shinoda, K.; Soda, T. *J. Phys. Chem.* **1963**, *67*, 2072.

(20) (a) Terabe, S.; Otsuka, K.; Ando, T. *Anal. Chem.* **1985**, *57*, 834. (b) Terabe, S.; Otsuka, K.; Ichikawa, K.; Tsuchiya, A.; Ando, T. *Anal. Chem.* **1984**, *56*, 111. (c) Kord, A. S.; Strasters, J. K.; Khaledi, M. G. *Anal. Chim. Acta* **1991**, *246*, 131. (d) Foley, J. P. *Anal. Chim. Acta* **1990**, *231*, 237. (e) *Capillary Electrophoresis: theory and practice*; Camilleri, P., Ed.; CRC Press: Boca Raton, FL, 1993.

(21) (a) Lee, B.-H.; Christian, S. D.; Tucker, E. E.; Scamehorn, J. F. *J. Phys. Chem.* **1991**, *95*, 360. (b) Dougherty, S. J.; Berg, J. C. *J. Colloid Interface Sci.* **1974**, *48*, 110.

(22) (a) Mukerjee, P.; Cardinal, J. R.; Desai, N. R. in ref 5e, Vol. 1, p 241. (b) Almgren, M.; Grieser, F.; Thomas, J. K. *J. Am. Chem. Soc.* **1979**, *101*, 279.

(23) Molecular models indicate that **1** and **2** would occupy ~15% and 3% respectively, of the volume of the hydrocarbon portion of an average SDS micelle. These calculations assume a radius of 18.4 Å for the hydrocarbon portion of the micelle, ref 24.

(24) Cabane, B.; Duplessix, R.; Zemb, T. *J. Physique* **1985**, *46*, 2161.

(25) Porphyrin-containing micelles persist well below the cmc of SDS (see ref 7b) since large hydrophobic solutes induce micelle formation: Law, K. Y. *Photochem. Photobiol.* **1981**, *33*, 799.

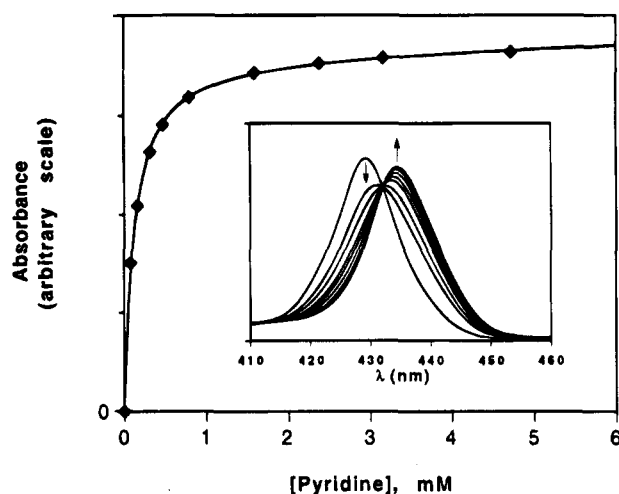


Figure 2. Typical UV binding isotherm for titration of **1** in 30 mM SDS with pyridine, with least squares fit to 1:1 isotherm. Insert: Soret band during titration showing isosbestic point.

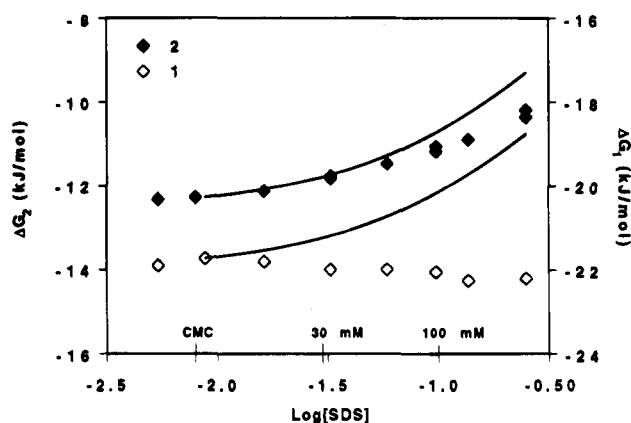


Figure 3. Pyridine binding energies for **1** and **2** as a function of SDS concentration. The solid curves starting from the cmc of SDS are binding energies calculated from eq 1 using $K_p(\text{pyridine}) = 40$ (Table 2).

species. **L1**–**L9** are assumed to reside largely in the outer region of micelles since there is much spectroscopic evidence that aromatic solutes experience polar environments inside micelles.^{17a,22} The deviations of **L10** and **L11** in Figure 4 may signal deeper penetration of these ligands, into a region more disrupted by the receptors.

In summary, the simplest binding model holds up well for most ligands, consistent with a common solubilization site for polar species. While extrapolation of binding energies measured at 100 and 30 mM SDS suggests that **1** and **2** would be best compared at SDS concentrations around the cmc, for practical reasons the equilibrium constants discussed below were measured at 30 mM SDS. However the difference between **1** and **2** at this concentration is small enough (~ 1 kJ/mol) that binding energies can still be meaningfully compared.

Recognition inside Micelles. The binding selectivity of **1** in a given solvent is best analyzed by comparison with **2**, defining a recognition energy $E_{\text{recog}} = \Delta G_1 - \Delta G_2$.¹⁰ In this way variations in zinc–nitrogen bond strength between different ligands and changes in ligand solvation both factor out, leaving

(26) Two pieces of indirect evidence suggests that **1** may have a more labile solubilization equilibrium, possibly leading to a thicker coating of surfactant at high SDS concentration. (1) The Soret λ_{max} of **1** blue shifts slightly with increasing SDS concentration, whereas the λ_{max} of **2** remains constant, and (2) ΔG_{obs} values for pyridine increase more for **1** than for **2** as ionic strength is increased. SDS micelles grow larger at high ionic strength: Kratochvil, J. J. *Colloid Interface Sci.* **1980**, *75*, 271.

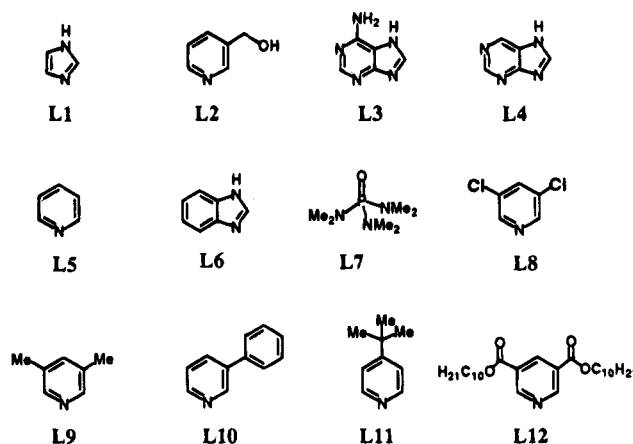


Table 2. Binding Energies (kJ/mol) in SDS

	$-\Delta G_{\text{obs}}^a$					
	1		2			
	30 mM	100 mM	30 mM	100 mM	K_p^b	$-\Delta G_p^c$ 30 mM
L1 ^d	15.1	16.4	12.1	11.8	9.2	5.3
L2	19.4	19.4	12.3	11.5	12	5.9
L3	18.9	19.6	9.8	9.0	20	7.1
L4	18.5	18.9	11.6	11.0	23	7.4
L5	22.0	22.0	11.8	11.1	40	8.5
L6 ^d	21.4	20.9	16.8	14.9	88	9.9
L7	25.0	25.3	3.2 ^e	1.7 ^e	89	9.9
L8	32.0	30.8	11.3	8.8	238	11.2
L9	33.8	32.6	15.8	12.6	670	11.9
L10	20.2 ^e	19.5 ^e	19.8 ^e	14.5 ^e	1835	12.2
L11	11.3 ^f	9.6 ^f	15.2 ^f	9.6 ^f	3010	12.3

^a By UV titration in 30 or 100 mM SDS (10 mM pH 7 buffer) at 295 K, errors ± 0.2 kJ/mol. ^b Partition coefficients by micellar capillary electrophoresis. ^c Partitioning energy in 30 mM SDS, $\Delta G_p = -RT \ln [K_p/(1 + ([\text{SDS}] - \text{cmc})/K_p - 1)]$. ^d 10 mM pH 9 buffer employed. ^e Errors ± 0.5 kJ/mol. ^f Errors ± 1.0 kJ/mol.

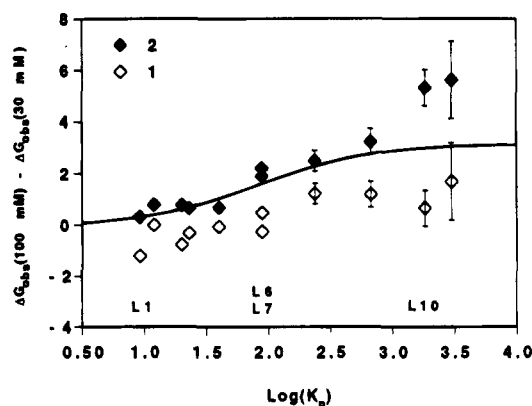


Figure 4. Difference between binding energies at 100 and 30 mM SDS and **1** and **2** as a function of ligand partition coefficient. The solid line is the difference from eq 1 using K_p values in Table 2.

only the extent to which the recognition site (roof) of **1** enhances binding, plus any difference in receptor solvation between **1** and **2**.

In CH_2Cl_2 ligands **L1**, **L2**, and **L6** which can form one hydrogen bond have recognition energies of -3.8 , -5 , and -6.1 kJ/mol, respectively, and **L3** and **L4** which can form two hydrogen bonds have $E_{\text{recog}} = -19.1$ and -15.3 kJ/mol (Table 3). van der Waals or dispersive interactions are generally weak in organic solvents, but ligands **L8** and **L9** which are the right size to contact the underside of the cap are attracted by $E_{\text{recog}} = -7$ kJ/mol. The bulky ligand **L11** which is too large to fit comfortably under the cap is repelled by $E_{\text{recog}} = +18$ kJ/mol.

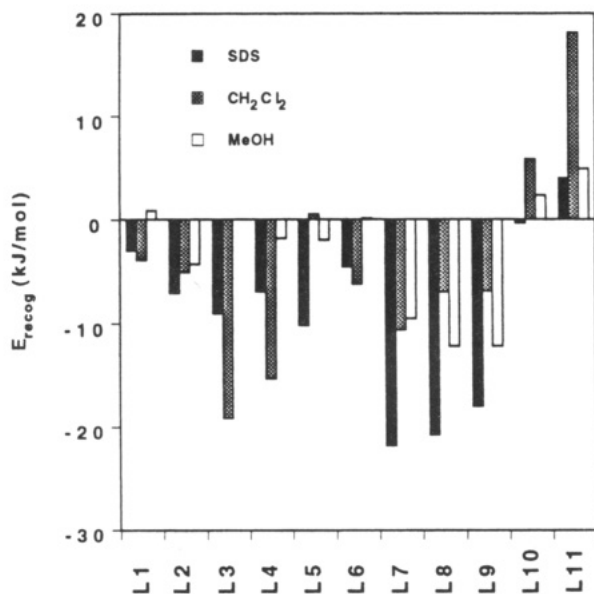


Figure 5. Trends in recognition energy, $E_{\text{recog}} = \Delta G_1 - \Delta G_2$ in 30 mM SDS, CH_2Cl_2 , and MeOH (Tables 2 and 3).

In SDS solution the use of recognition energies also factors out differences in partition coefficient between ligands. E_{recog} values in SDS, methanol, and CH_2Cl_2 are displayed in Figure 5. Compared to CH_2Cl_2 , two main trends are apparent: hydrogen bonding is weaker inside micelles and solvophobic binding is stronger.²⁷ Recognition of one-hydrogen-bond ligands is largely unaffected, but recognition of two-hydrogen-bond ligands is decreased in SDS by on average 9 kJ/mol relative to CH_2Cl_2 . For closely fitting ligands **L8** and **L9** recognition is increased by 12.5 kJ/mol, and for the oversized ligand **L11** recognition is increased by 14.2 kJ/mol.

Intramolecular Binding Energies. Receptor and Ligand Solvation in SDS and Methanol. Subtraction of ligand partitioning energies from observed binding energies (Table 2) gives absolute intramolecular binding energies, $\Delta G_i = \Delta G_{\text{obs}} - \Delta G_p$. In 30 mM SDS ΔG_i values for **1** range from +1 to -22 kJ/mol (K_i from 0.7 to 7900 M^{-1}), with ligand-micelle partitioning accounting for ~40% of the experimentally measured energies for **L1** to **L9** and most of the binding energy for the more hydrophobic ligands **L10** and **L11**. Binding energy in solution is determined by the difference in solvation energy of the initial and final states in addition to the intrinsic or gas phase binding energy, so comparison of two receptors (**1** and **2**) binding the same set of ligands (**L1**–**L11**) in two solvents (SDS and MeOH) allows comparison of ligand and receptor solvation in micelles and methanol.

A difference in recognition energy for a given ligand in two solvents is independent of ligand solvation but includes differences in receptor solvation.²⁸ Recognition energies in SDS and MeOH change roughly in parallel (Figure 5), and a plot of $E_{\text{recog}}(\text{SDS})$ versus $E_{\text{recog}}(\text{MeOH})$ (supporting information, $R = 0.96$) shows that recognition energies are on average 4 kJ/mol larger in SDS than in methanol. This is interpreted as a cavity solvation effect; despite heavier hydration of **1** than **2** by water in micelles, the steroidal superstructure on balance protects the binding site of **1** by excluding the large surfactant chains more

effectively than it excludes methanol. Cavity solvation effects are characteristic of **1**, with E_{recog} for pyridine varying by more than 10 kJ/mol in different organic solvents (see below).

A difference in absolute binding energy for a given ligand in two solvents is determined by differences in both ligand and receptor solvation. Since the difference in receptor solvation between SDS and methanol is known, comparisons of intramolecular binding energies allows comparison of ligand solvation in these two media. A plot of ΔG_i values against binding energies in methanol is shown in Figure 6. Considering the ligands as a set, ligands bind on average 5.3 kJ/mol more strongly to **1** than to **2** in SDS compared to methanol. Thus ligand solvation is on average $5.3 - 4 = 1.3$ kJ/mol less favorable in SDS than in methanol.

In CH_2Cl_2 cavity solvation inhibits binding slightly, by ~1 kJ/mol relative to **2**,²⁹ so recognition energies in SDS are intrinsically larger than in CH_2Cl_2 by $4 + 1 = 5$ kJ/mol. Hence in absolute terms the binding of two-hydrogen-bond ligands is reduced in SDS by $\sim 9 + 5 = 14$ kJ/mol relative to CH_2Cl_2 , and binding of one-hydrogen-bond ligands is reduced by ~5 kJ/mol. Binding of well matched ligands **L8** and **L9** is increased by ~7.5 kJ/mol, and binding of **L11** is increased by ~9 kJ/mol. This large enhancement for **L11**, which is a very weakly binding species in CH_2Cl_2 , is presumably due to the large area of hydrocarbon contact provided by the *tert*-butyl group.

Given the approximations involved in factoring solvation energies, and the slight deviation of **1** from eq 1 at 30 mM SDS, the figures above should be regarded as semiquantitative estimates. Nevertheless the main conclusions are clear: (1) the superstructure of **1** protects the binding site more effectively in SDS than in methanol, (2) ligand solvation energies are similar in SDS and methanol, (3) solvophobic binding is much enhanced in SDS compared to CH_2Cl_2 , and (4) hydrogen bonding is much reduced in SDS compared to CH_2Cl_2 . This last point agrees with results of Nowick et al., who estimated $K_i \sim 1 \text{ M}^{-1}$ for base pairing inside SDS micelles compared to $K \sim 40 \text{ M}^{-1}$ in chloroform.^{6a}

Methanol-like ligand solvation energies are consistent with solubilization near the surface of SDS micelles and are also in line with a recent analysis of K_p values showing that for many small solutes the SDS pseudophase has the hydrophobic character of water-saturated isobutyl alcohol.³⁰ Particularly hydrophobic ligands would be expected to bind more strongly to a core-dwelling receptor. In fact there is little sign of this effect in Figure 6, with equal scatter of hydrophobic and hydrophilic species for both porphyrins. This suggests that while ligands may indeed localize in preferred regions within an SDS micelle, the energy differences within such a dynamic disordered environment are not large, and hydrophilic species can easily find the receptor. Methanol-like absolute binding energies are also consistent with an appreciable degree of receptor hydration.

Chiral Recognition inside Micelles. Modulation of Enantioselectivity. In CH_2Cl_2 **1** discriminates well between the enantiomers of small amino acid derivatives capable of forming two hydrogen bonds, such as serine methyl ester **L13**. Bulkier or less functionalized amino acids **L15** and **L16** are bound less enantioselectively, Table 4. A large downfield shift of the OH doublet of **1** on ^1H NMR titration with **L15** (CDCl_3) shows that the ester group of a zinc-bound substrate is capable of hydrogen bonding to one or more roof hydroxyl groups:

(27) The term solvophobic is used here to indicate that nonpolar contacts are more favorable in polar solvents because solvation raises the energy of the initial state more than the final state, with the dispersive contribution being to a first approximation independent of solvent.

(28) Strictly speaking this also includes terms due to complex solvation. Differences in solvation of the empty receptor are assumed to be more important.

(29) Solvation of **1** relative to **2** in CH_2Cl_2 is estimated from the binding of small species which do not interact with the roof of **1**: $E_{\text{recog}}(\text{isooxazole}) = 1.1 \text{ kJ/mol}$.

(30) Abraham, M. H.; Chadha, H. S.; Dixon, J. P.; Rafols, C.; Treiner, C. *J. Chem. Soc., Perkin Trans. 2* **1995**, 887.

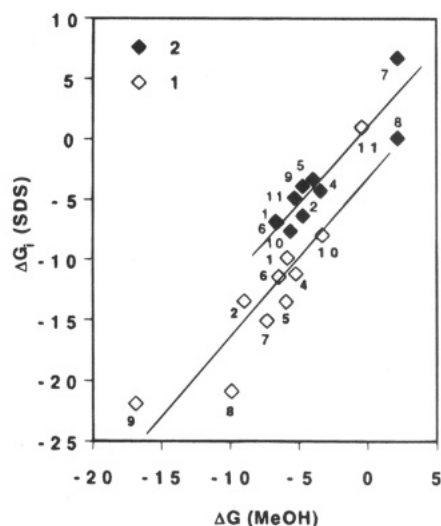


Figure 6. Correlation between binding energies inside SDS micelles (ΔG_i) and binding energies in methanol (Tables 2 and 3). The separation between the least squares fits ($R = 0.91$ for **2** and $R = 0.90$ for **1**) is 3.7 kJ/mol. In SDS the average ligand binding energy to **1** is -12.4 kJ/mol and to **2** is -3.6 kJ/mol. In methanol the average binding energy to **1** is -7 kJ/mol and to **2** is -3.6 kJ/mol.

Table 3. Binding Energies (kJ/mol) in CH_2Cl_2 and MeOH

	$-\Delta G_{\text{obs}}^a$			
	CH_2Cl_2		MeOH	
	1	2	1	2
L1	31.9	28.1	5.8	6.7
L2	29.2	24.2	9.0	4.7
L3 ^b	42.3	23.2		
L4	35.7	20.4	5.2	3.4
L5	23.8	24.3	5.9	3.9
L6	32.4	26.3	6.4	6.6
L7	29.4	18.7	7.3	-2.2^c
L8	22.4	15.4	9.9	-2.2^c
L9	31.8	24.9	16.9	4.7
L10	18.1	23.9	3.3	5.6
L11	7.6	25.7	0.4 ^d	5.3

^a By UV titration in dry organic solvent at 295 K, errors ± 0.2 kJ/mol. ^b Measured in CH_2Cl_2 containing 0.5% v/v MeOH due to low ligand solubility. ^c Errors ± 1.0 kJ/mol. ^d Errors ± 0.5 kJ/mol.

interaction of the side chain with the C_2 -chiral superstructure then provides for three point recognition. As shown in Figure 7 enantioselectivity, defined as $E_{\text{L/D}} = \Delta G_{\text{L}} - \Delta G_{\text{D}}$, changes in parallel with average recognition energy $E_{\text{recog}}(\text{D/L average})$, where $E_{\text{recog}}(\text{D/L average})$ is the difference between the average binding energy of ligand enantiomers to **1** and their binding energy to **2**. A correlation with enantioselectivity implies that **1** functions by binding one enantiomer particularly strongly, rather than binding the other enantiomer unusually weakly (if $E_{\text{recog}}(\text{D/L average}) \approx 0$ then one enantiomer would be repelled as much as the other was attracted).

In SDS micelles the trend is similar, but with the maximum in both $E_{\text{L/D}}$ and $E_{\text{recog}}(\text{D/L average})$ shifted toward more hydrophobic ligands. $E_{\text{L/D}}$ is increased by 5.3 kJ/mol for threonine (from 53 to 93% ee) and 2.1 kJ/mol for valine (from 12 to 50% ee) but reduced by 1.4 kJ/mol (from 86 to 76% ee) for serine (enantiomers are being compared, so partitioning effects cancel). Weaker hydrogen bonding accounts for the drop in enantioselectivity for serine. Methyl group contacts for threonine and valine are evidently sufficiently enhanced inside the micelle to override any reduction in hydrogen bond strength. Complexes of **1** with D and L enantiomers are slightly different colours due to different Soret λ_{max} s and extinction coefficients.

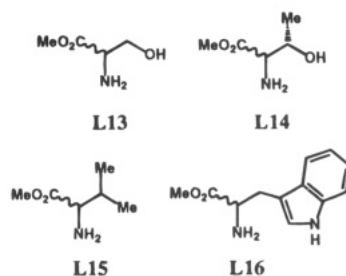


Table 4. Binding Energies (kJ/mol) for Amino Acid Methyl Esters in SDS and CH_2Cl_2

	$-\Delta G$			
	SDS		CH_2Cl_2	
	1	2	1	2
L-L13	18.7	8.9	31.1	19.5
D-L13	13.8		24.8	
L-L14	30.1	12.6	29.0	19.3
D-L14	21.9		26.1	
L-L15	28.9	15.8	25.1	23.2
D-L15	26.2		24.5	
L-L16	27.3	20.3	23.0	26.9
D-L16	26.5		22.7	

^a By UV titration in 30 mM SDS (100 mM pH 9 buffer) or dry CH_2Cl_2 at 295 K, errors ± 0.2 kJ/mol.

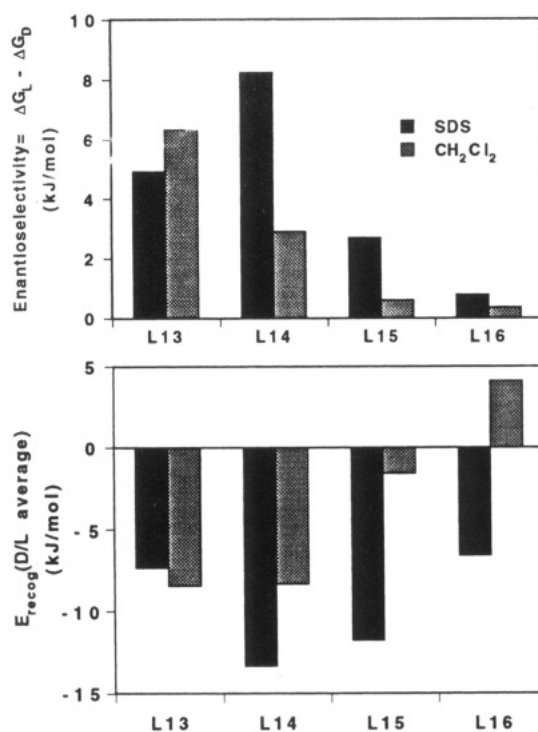


Figure 7. Enantioselectivities and average recognition energies of amino acid methyl esters in 30 mM SDS and CH_2Cl_2 . $E_{\text{recog}}(\text{D/L average}) = (\Delta G_{\text{1D}} + \Delta G_{\text{1L}} - 2\Delta G_{\text{2L}})/2$ (Table 4).

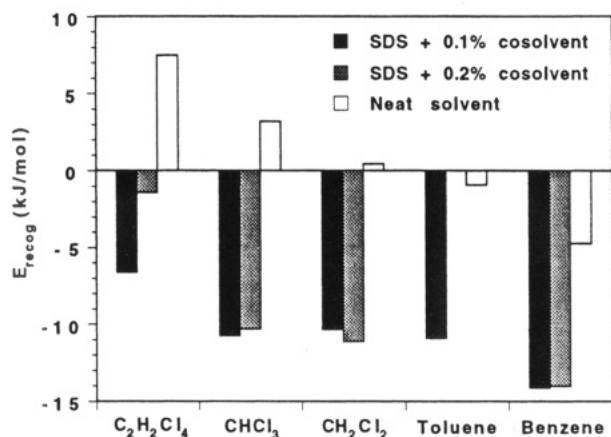
Solvent Engineering inside Micelles. Effects of Added Cosolvent. Micellar receptors would be more versatile if overall ligand selectivities could be altered, either by changing the partitioning properties of the micellar phase or changing the intrinsic selectivity of the receptor. Different surfactants have different K_p values for a given ligand, but relative K_p values for different ligands do not vary much with surfactant,³¹ so the approach was to take advantage of cavity solvation effects and

(31) (a) Treiner, C.; Mannebach, M.-H. *J. Colloid Interface Sci.* **1987**, *118*, 243. (b) Mukerjee, P.; Ko, J.-S. *J. Phys. Chem.* **1992**, *96*, 6090. (c) Stilbs, P. *J. Colloid Interface Sci.* **1983**, *94*, 463.

Table 5. Pyridine Binding Energies (kJ/mol) in SDS with Added Cosolvents

cosolvent		$-\Delta G^a$			
		SDS + cosolvent		neat solvent	
		%v/v		1	2
C ₂ H ₂ Cl ₄	0.1		22.5	15.9	15.4
	0.2		21.5	20.1	22.9
CHCl ₃	0.1		23.6	12.9	19.6
	0.2		24.3	14	22.9
CH ₂ Cl ₂	0.1		22.6	12.3	23.8
	0.2		23.8	12.7	24.3
toluene	0.1 ^b		25.9	14.9	24.1
benzene	0.1		27.5	13.3	28.8
	0.2		28.3	14.3	24.1

^a By UV titration in dry organic solvents or in 30 mM SDS (10 mM pH 7 buffer) at 295 K, errors ± 0.2 kJ/mol. ^b Only 0.1 v/v toluene could be solubilized in 30 mM SDS.

**Figure 8.** Recognition energies for pyridine in 30 mM SDS containing 0.1 or 0.2% v/v organic solvent and in neat organic solvents (Table 5).

change the binding selectivities of **1** and **2** inside micelles by altering the local solvent environment.

Addition of various organic solvents to **1** or **2** in 30 mM SDS gave homogenous, optically clear solutions with small changes in Soret λ_{\max} (± 1.5 nm). Pyridine binding energies for solutions containing 0.1 and 0.2% v/v organic solvent are in Table 5. All added cosolvents increase binding, although by different amounts for **1** and **2**. As shown in Figure 8 there is a parallel between recognition energies in solvent-doped micelles and in neat organic solvents, E_{recog} decreasing in both media on going from tetrachloroethane to benzene. This shows that solvation of a receptor inside a micelle can be tuned to take on the characteristics of an organic solvent. An exact parallel is not expected since the cosolvents have different partition coefficients and may prefer different regions inside the micelle.^{31a}

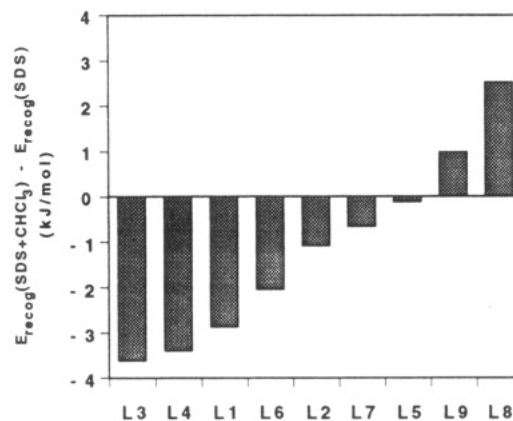
Binding energies for **L1**–**L9** are given in Table 6 for solutions containing 0.2% v/v chloroform.³² Added cosolvent again results in stronger overall binding, increasing ΔG_{obs} by different amounts for **1** and **2**. The differences between E_{recog} values with and without chloroform are shown in Figure 9. Recognition of two-hydrogen-bond species **L3** and **L4** is enhanced the most, followed by one-hydrogen-bond ligands, and recognition of the dispersive binders **L8** and **L9** is reduced. Thus hydrogen bonding can be partially restored by organic cosolvents, and solvophobic forces weakened, allowing some control over binding selectivities. The partition coefficients measured by capillary electrophoresis for **L4**, **L5**, and **L9** were virtually

(32) A concentration of 0.2% v/v chloroform in 30 mM SDS corresponds to ~ 0.5 M chloroform in the micellar phase. $K_p(\text{chloroform}) = 38$, $K_p(\text{benzene}) = 93$, $K_p(\text{toluene}) = 307$. Cosolvent partition coefficients are taken from ref 31a.

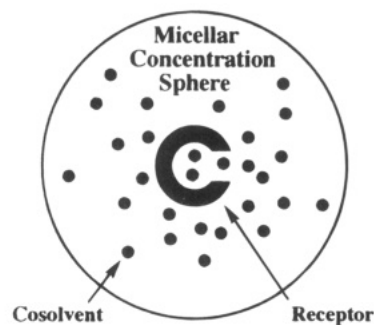
Table 6. Binding Energies (kJ/mol) in Chloroform-Doped Micelles

	$-\Delta G^a$	
	1	2
L1	18.6	12.7
L2	21.2	13.1
L3	23.4	10.7
L4	22.8	12.5
L5	24.3	14
L6	24.1	17.6
L7	27.1	4.7
L8	34.1	15.8
L9	35.1	18.1

^a By UV titration in 30 mM SDS (10 mM pH 7 buffer) containing 0.2% v/v chloroform at 295 K, errors ± 0.2 kJ/mol.

**Figure 9.** The effect of added chloroform (0.2% v/v) on recognition energies in 30 mM SDS (Table 6).

unchanged by the addition of 0.2% v/v chloroform suggesting that chloroform is solubilized in the core of micelles and changes in binding energy are mainly due to changes in receptor solvation. The main features of recognition in solvent-doped micelles are summarized pictorially below.



Summary and Concluding Remarks

Micellar inclusion turns out to be a simple and direct method for introducing an otherwise completely insoluble receptor into water. Despite the potential complexity of recognition inside a dynamic surfactant assembly, ligand binding in SDS was surprisingly well behaved, suggesting that this approach should be extendible to other water-insoluble receptors which currently function only in organic solvents—particularly those with partially enclosed binding sites. Comparisons of **1** and **2** showed that the reference porphyrin had little effect on “normal” micellar behavior, but the introduction of bulky receptor **1** did produce deviations at high surfactant concentrations. However the energetic consequences for ligand recognition were small since, in keeping with the pseudophase approximation, ligand-micelle partitioning was quite insensitive to the presence of **1** or indeed

to relatively high concentrations of ligand or cosolvent in the micellar phase.

Binding inside SDS micelles was found to be energetically similar to binding in methanol, except that the roof of **1** provides more protection for the binding site in SDS. Binding of two-hydrogen-bond ligands was reduced by ~ 14 kJ/mol relative to CH_2Cl_2 in absolute terms (or ~ 9 kJ/mol if receptor solvation is not included) and by ~ 5 kJ/mol for one-hydrogen-bond ligands. The solvophobic effect provided a significant driving force for recognition, increasing binding of ligands capable of contacting the hydrocarbon roof by ~ 8 kJ/mol. Intramicellar recognition was particularly effective when hydrogen bonding and solvophobic interactions acted cooperatively. Thus a single methyl group contact was enough to boost the recognition energy of the threonine derivative **L14** in micelles relative to organic solution, providing the highest enantioselectivity reported for this class of ligand.³³

A micellar receptor is effectively restricted to a small volume by the converging surfactant chains, allowing its solvent environment and hence recognition properties to be tuned by doping with small amounts of nonpolar solvents. Recognition energies could be varied over a range of 12.5 kJ/mol, and the balance between hydrogen bonding and solvophobic interactions was altered. Such "solvent engineering" in microheterogeneous aqueous solution seems unprecedented.³⁴ Chiral micellar receptors might find uses as sensors for species in aqueous solution—**1** gave visible color changes at mM to μM ligand concentrations. Other possible applications include the chiral version of micellar chromatography^{20e} and as catalysts for reactions in which turnover is ensured by favorable reactant and product partitioning.

Appendix

Derivation of the Concentration Factor F . The pseudophase or two phase model of micellar solubilization assumes that micelles can be notionally coalesced and treated as a separate, homogeneous phase.¹⁷ To analyze the general situation in which not all micelles contain receptor, the two phase treatment of Nowick et al.^{6b} is extended to a three phase model. Ligand is assumed to partition between the aqueous phase (volume V_{aq} , ligand concentration L_{aq}), a micellar phase which contains receptor (volume V_{mr} , ligand concentration L_{mr} , and partition coefficient $K_{\text{pr}} = L_{\text{mr}}/L_{\text{aq}}$), and an "empty" micellar phase which does not contain receptor (volume V_{m} , ligand concentration L_{m} , and partition coefficient $K_{\text{p}} = L_{\text{m}}/L_{\text{aq}}$). Material balance gives

$$L_0 V_t = L_{\text{aq}} V_{\text{aq}} + L_{\text{mr}} V_{\text{mr}} + L_{\text{m}} V_{\text{m}}$$

where V_t is the total volume of the system and L_0 is the bulk concentration of added ligand. Substituting for L_{aq} and L_{m} and rearranging gives

$$L_{\text{mr}} = L_0 K_{\text{pr}} / \{ V_{\text{aq}}/V_t + K_{\text{pr}} V_{\text{mr}}/V_t + K_{\text{p}} V_{\text{m}}/V_t \}$$

Defining phase volume ratios $\beta = V_{\text{m}}/V_t$ and $\beta_r = V_{\text{mr}}/V_t$ and using $V_{\text{aq}}/V_t = 1 - \beta - \beta_r$ gives

$$F = L_{\text{mr}}/L_0 = K_{\text{pr}} / \{ 1 + \beta_r (K_{\text{pr}} - 1) + \beta (K_{\text{p}} - 1) \}$$

In this expression K_{pr} appears in the numerator since only that fraction of micelles containing receptor is being monitored during titrations, and K_{p} appears in the denominator because ligand can also partition into empty micelles, reducing the concentration of ligand in the receptor phase. Measurement of K_{p} and K_{pr} using micellar capillary electrophoresis at SDS concentrations around 8 mM (see Experimental Section for details) showed that within experimental error $K_{\text{pr}} = K_{\text{p}}$, i.e., the presence of a receptor inside a micelle does not effect ligand-micelle partitioning at low surfactant concentrations. If only a small fraction of micelles contain receptor, then at SDS concentrations much above the cmc β_r can be neglected and the expression simplifies to

$$F = K_{\text{p}} / \{ 1 + \beta (K_{\text{p}} - 1) \}$$

where $\beta = ([\text{SDS}] - \text{cmc})v^{\text{m}}$ if the volume of the added ligand is small compared to V_{m} and V_t . If ligand partitioning is treated as a multiple equilibrium process¹⁸ with bimolecular equilibrium constant K_c a similar expression is obtained with the $K_{\text{p}} - 1$ term replaced by K_{p} . K_{p} is related to K_c by $K_c = Nv^{\text{m}}K_{\text{p}}\beta/(1 - \beta)$ where N is the aggregation number.

Experimental Section

General Methods. Surfactants were used as received. SDS was Sigma, 99%. All solutions and buffers were prepared in Milli-Q water. "10 mM pH 7 buffer" was 10 mM in total salts (6.1 mM Na_2HPO_4 , 3.9 mM NaH_2PO_4) and "10 mM pH 9 buffer" refers to 10 mM sodium tetraborate. UV-visible spectra were recorded on a Perkin-Elmer Lambda 2 instrument in 1 cm cells in a thermostatted cell holder at 295 K. ^1H NMR spectra and relaxation times were measured on a Bruker AM-400 at ambient temperature. Capillary electrophoresis was performed on an Applied Biosystems 270-HT instrument.

Ligands. Liquids were distilled before use, and 4-*tert*-butylpyridine (**L11**) was fractionated twice. Benzimidazole (**L6**) and adenine (**L3**) were recrystallized from water and purine (**L4**) from toluene. Commercially available L and D amino acid methyl ester hydrochlorides (Sigma) were dissolved directly in buffered SDS for titrations and used immediately. Noncommercially available D methyl ester hydrochlorides were prepared from the amino acid (10% w/w HCl in dry methanol, 12–48 h, followed by evaporation under high vacuum) as slowly crystallizing hygroscopic oils and were checked by ^1H NMR (D_2O) before use. For titrations in CH_2Cl_2 , free bases were generated from hydrochlorides either by stirring with K_2CO_3 in CH_2Cl_2 followed by filtration or by extraction from the minimum volume of saturated sodium hydrogen carbonate with chloroform and were checked by ^1H NMR (CDCl_3) and used immediately. The bisdecyl ester of dinicotinic acid **L12** was prepared as follows: 2,6-dichlorobenzoyl chloride (650 mg, 3.1 mmol) was added to a stirred solution of pyridine-3,5-dicarboxylic acid (250 mg, 1.5 mmol) and triethylamine (450 μL , 3.2 mmol) in dry THF (2.0 mL) at room temperature. After 1 h, decanol (475 mg, 3.0 mmol) was added followed by *N,N*-dimethylaminopyridine (50 mg), and the yellow suspension was stirred for 36 h. Workup with diethyl ether followed by chromatography (5% EtOAc in hexane) gave the bisdecyl ester as a colorless oil (445 mg, 66%): ^1H NMR (CDCl_3 , 250 MHz) 0.87 (brt, 6H), 1.2–1.5 (m, 28H), 1.78 (m, 4H), 4.37 (t, $J = 7$, 4H), 8.84 (t, $J = 1.8$, 1H), 9.35 (t, $J = 1.8$, 2H). Anal. Calcd for $\text{C}_{27}\text{H}_{45}\text{NO}_4$: C, 72.44; H, 10.13; N, 3.13. Found: C, 72.78; H, 10.29; N, 3.00.

Micellar Porphyrins. A two-phase mixture of aqueous surfactant (20 mL, 50–250 mM in surfactant and 10 mM in pH 7 buffer) and a

(33) Mitzutani, T.; Ema, T.; Tomita, T.; Kurada, Y.; Ogoshi, H. *J. Am. Chem. Soc.* **1994**, *116*, 4240.

(34) There are some parallels, in an inverse sense, with recent work on the properties of enzymes suspended in organic solvents where it has been shown that substrate specificity can be determined by partitioning effects and also modulated by addition of small quantities of water to the organic phase: (a) Westcott, C. R.; Klivanov, A. M. *J. Am. Chem. Soc.* **1993**, *115*, 1629. (b) Yang, Z.; Zacherl, D.; Russell, A. J. *J. Am. Chem. Soc.* **1993**, *115*, 12251. (c) Wangikar, P. P.; Greycar, T. P.; Estell, D. A.; Clark, D. S.; Dordick, J. S. *J. Am. Chem. Soc.* **1993**, *115*, 12231.

(35) Harada, S.; Okada, H.; Sano, T.; Yamashita, T.; Yano, H. *J. Phys. Chem.* **1990**, *94*, 7648.

(36) (a) Gao, Z.; Wasylshen, R. E.; Kwak, J. C. T. *J. Phys. Chem.* **1989**, *93*, 2190. (b) Gao, Z.; Wasylshen, R. E.; Kwak, J. C. T. *J. Chem. Soc., Faraday Trans.* **1991**, *87*, 947.

dichloromethane solution of porphyrin (4 mL, 5 to 500 μM in porphyrin) was sonicated in a Pyrex tube (2.5×10 cm) for 1 min, cooling the tube in an ice-bath. The sonicator probe (a Heat Systems-Ultrasonics W-375 microprobe, tuned in air at maximum power setting) was inserted almost to the bottom of the tube, and its position was adjusted to produce rapid vortexing of the mixture. After sonication the thick creamy suspension was stirred rapidly under a flow of argon, warming the bottom of the tube in a water bath at 40 $^{\circ}\text{C}$ until the organic solvent had evaporated (~ 30 min, slight foaming). The tube was then immersed further into the water bath, and stirring continued at 40 $^{\circ}\text{C}$ for 1 h. The solutions thus obtained were left in the dark at room temperature for 2–4 days before use, during which time the porphyrin Soret bands sharpened slightly and settled to constant λ_{max} . Filtration through a 0.2 μm filter produced no change in absorbance. Solutions of (monomeric) **1** in SDS were greenish-orange, changing to a more intense bluish-green on addition of amine ligands. An alternative method involving slow addition of a solution of porphyrin in THF or acetone to warm, rapidly stirred aqueous SDS was also effective.

Solutions of **1** in SDS with sharp symmetrical Sorets, $\lambda_{\text{max}} = 429.5$ nm (measured at 30 mM SDS) were reliably obtained provided that the [surfactant]/[porphyrin] ratio $R \geq 10^4$. Solubilization with $R < 100$ produced asymmetric red-shifted Sorets with λ_{max} up to 434 nm. Titrations of these red-shifted preparations with pyridine were not isosbestic and did not fit 1:1 binding isotherms well. Addition of more surfactant so that $R \geq 10^4$ and reprocessing with organic solvent gave solutions with identical properties to those initially prepared with $R \geq 10^4$. **2** gave predominantly blue-shifted preparations when $R < 100$. These effects are likely due to porphyrin aggregation, with red or blue shifts signaling edge-to-edge or face-to-face aggregation, respectively.^{7b} C_{60} , which has a large hydrocarbon surface like **1**, also aggregates in micelles and bilayers.⁹ Samples of monomeric **1** and **2** in 100 mM SDS appeared essentially unchanged after storage in the dark at room temperature for more than 6 months, as judged by UV spectra and K_{obs} values for pyridine. All K_{obs} values in this paper were determined for strictly monomeric **1** and **2** as determined by λ_{max} values and quality of fit to 1:1 binding isotherms. K_{obs} values were reproducible from batch to batch to within $\pm 15\%$ for **1** and $\pm 10\%$ for **2**.

Solutions in which every micelle contains a receptor could be produced by dialysis or simply by dilution below the cmc.²⁵ For capillary electrophoresis experiments, the concentration of excess surfactant was reduced by dialysis of 10 mL samples (cellulose bags, Visking) against pure water (1 L), changing the water at 12 h intervals. The concentration of SDS in the dialysis bag was determined by ^1H NMR integration of lyophilized aliquots, adding methanol as an internal standard. Extended dialysis of solutions of **1** containing < 1 mM SDS eventually resulted in porphyrin aggregation and some loss of porphyrin.

UV–Visible Titrations. For a typical titration in 30 mM SDS, 275 μL of a stock solution of micellar **1** (250 mM in SDS, 10 mM in pH 7 buffer, 5 μM in **1**) was added to 2.0 mL of 10 mM in pH 7 buffer in a cuvette to give an absorbance of ca. 0.5. A concentrated solution of ligand in 30 mM SDS (10 mM in pH 7 buffer) was then added in portions with a microsyringe, monitoring at four or six wavelengths around the Soret bands of free and bound receptor. For routine titrations 10–15 ligand additions were made, covering 0–95% of the binding isotherm, ligand solubility and equilibrium constant permitting, and volume changes were taken into account during analysis. For isosbestic point checks at constant porphyrin concentration, the ligand solution was made up with the same porphyrin solution as in the cuvette. For titrations in solvent-doped micelles, organic cosolvents were added directly to the cuvette, stirring until the Soret band had settled to constant λ_{max} and an optically clear solution was obtained. K_{obs} values for enantiomeric amino acid esters binding to **2** agreed to better than 15%. 10 mM pH 7 phosphate was found to be sufficient to buffer pyridine titrations, producing negligible change in bulk pH as measured with a pH meter: pyridine titrations in 10 mM pH 10 buffer gave the same K_{obs} values as at pH 7.

Equilibrium constants were calculated from absorbance changes as previously described.^{10b} Briefly, K_{obs} values were obtained by curve fitting to $A_{\text{exp}} = A_i + (A_f - A_i)K_{\text{obs}}L_0/(1 + K_{\text{obs}}L_0)$ treating A_f and K_{obs} as unknowns, where A_{exp} is the experimental absorbance, and A_i and A_f are the initial and final absorbancies. For K_{obs} values greater than

$\sim 5 \times 10^4 \text{ M}^{-1}$ the full binding quadratic was used. For very low equilibrium constants in methanol and SDS ($K_{\text{obs}} < 5 \text{ M}^{-1}$), high ligand concentrations began to induce deviations from isosbesticity, red-shifting the porphyrin chromophore by amounts proportion to the ligand concentration. To correct for this effect **1** and **2** were titrated to $\leq 50\%$ saturation, and absorbance values were determined at wavelengths around the Soret band half-heights to ensure that small band displacements lead to linear corrections.

The kinetics of **L12** binding to **1** were measured by following the absorbance changes at four wavelengths in 100 mM SDS at 295 K. Enough ligand was added initially to produce $\sim 30\%$ bound receptor at equilibrium, ensuring that absorbance readings were taken over an essentially linear part of the binding isotherm. K_{obs} for **L12** was estimated as $\sim 2 \times 10^6 \text{ M}^{-1}$ by adding ligand to a series of solutions containing micellar **1** in disposable cuvettes and recording absorbances after 40 h. This value may be an overestimate due to the effects of micellar saturation. Solutions of **L12** in 100 mM SDS were prepared using the ultrasonic emulsification method. Cloudy suspensions were obtained when $[\text{L12}] \geq 10 \text{ mM}$ suggesting ≥ 10 molecules of surfactant per ligand at saturation.

Ligand Partition Coefficients. Micellar capillary electrophoresis was performed essentially as described by Terabe et al.^{20a,b} with an uncoated 75 μm , 70 cm long silica capillary. The column temperature was 27 $^{\circ}\text{C}$, voltage 25 kV, current 20–40 μA , and detection was by UV at 200 nm. Ligand solutions (1–5 μL , 2–10 mg/mL in the mobile phase, or saturated solutions for the less soluble ligands) were added successively to 200 μL of the mobile phase in the source vial, running a chromatogram after each addition to identify the peaks. Dodecyl-oxybenzene or **H2** were used as markers to measure the micelle retention time (t_m). After the ligands and the micelle marker had been added, the solvent front time (t_0) was obtained by adding enough methanol to the mixture (1–2% v/v) to produce a detectable inflection in the baseline. Provided the amount of methanol added was small, the retention times of ligands and marker were not significantly effected. K_p values were calculated from $K_p = k/([\text{SDS}] - \text{cmc})v^m$, where the capacity factor $k = (t_r/t_0 - 1)/(1 - t_r/t_m)$ and t_r is the ligand retention time. In the absence of surfactant not all of the ligands had identical mobilities, but most coeluted with methanol as an unresolved peak. The partition coefficients in Table 2 were measured in 100 mM SDS containing 10 mM pH 7 buffer (or 10 mM pH 9 buffer for imidazole ligands **L1** and **L6**). At this surfactant and buffer concentration relative K_p values were repeatable to better than 15%. A plot of capacity factor versus SDS concentration (10, 20, 40, 60, 80, and 100 mM at 50 mM pH 7 buffer) for ligands **L5** and **L9** gave good straight lines. In an attempt to distinguish the K_p and K_{pr} terms in the expression for the concentration factor F (Appendix), partition coefficients for **L4**, **L5**, and **L9** were measured using mobile phases containing a constant concentration of **H21** or **H22** (34 μM) and SDS concentrations of 4, 8, 12, and 16 mM (all 10 mM in pH7 buffer) such that the fraction of porphyrin-containing phase varied from $\beta_f/\beta \approx 1$ to $\beta_f/\beta \approx 0.2$. The free base porphyrins were used to avoid changes in apparent K_p values due to receptor-ligand binding. There were no significant differences in retention time in the presence of **H21** or **H22** or when porphyrin was not included. The effect of organic cosolvents on partition coefficients was measured by first running a mixture of **L4**, **L5**, and **L9** plus marker in a mobile phase of 30 mM SDS containing 10 mM pH 7 buffer, then running the same mixture in a mobile phase in which 0.2% v/v of chloroform or dichloromethane had been dissolved, and finally switching back to the first mobile phase. Apart from large negative peaks due to cosolvent, there were only minor differences in retention times in the presence and absence of cosolvent.

Attempts to measure ligand K_p values by ^1H NMR titration of ligand with SDS or *vice versa* gave erratic results, apparently because small variations in the extent of amine protonation were sufficient to swamp the small differences in chemical shift involved.³⁵

Partition coefficients could however be measured by the paramagnetic relaxation method of Kwak et al.³⁶ Longitudinal relaxation times were measured for 6 mM ligand in pH 9.5 carbonate buffer (10 mM total salts) in the presence and absence of 25 mM SDS and 1 mM 3-carboxypropyl (Aldrich). Peak heights from inversion recovery experiments (12–15 delays) were analyzed with standard Bruker software. Only the *para*-proton T_1 's were used to calculate K_p values

due to anomalous relaxation (broadening) of the *ortho*, and to some extent the *meta*, protons on micellar solubilization.³⁵ Values for **L5**, $K_p = 60 (\pm 20)$ and for **L2**, $K_p = 18 (\pm 5)$ are slightly higher than those found by capillary electrophoresis, but in reasonable qualitative agreement given the different temperatures, solvents, and buffers involved.

Acknowledgment. Thanks to Christ's College Cambridge for financial support, Dr. Jeremy Sanders for his encouragement, Dr. Daniel Horowitz and Dr. Steven Wylie for useful suggestions, and Prof. Alan Fersht for use of the capillary electrophoresis instrument.

Supporting Information Available: UV data for **1** and **2** in organic solvents (Figure 1A,B), pyridine binding energies as a function of SDS concentration (Figure 3), and correlation between $E_{\text{recog}}(\text{SDS})$ and $E_{\text{recog}}(\text{MeOH})$ for **L1–L11** (3 pages). This material is contained in many libraries on microfiche, immediately follows this article in the microfilm version of the journal, can be ordered from the ACS, and can be downloaded from the Internet; see any current masthead page for ordering information and Internet access instructions.

JA952342O